Chem. Pharm. Bull. Regular Article

Synthesis of 2,8-Dioxabicyclo[3.3.1]nonane Derivatives and their Neuroprotective Activities

Hitoshi Kamauchi[a]*, Masafumi Takanashi[a], Mitsuaki Suzuki[b], Kouki Izumi[a], Koichi Takao[a] *and* Yoshiaki Sugita[a]

[a]*Department of Pharmaceutical Sciences, Faculty of Pharmacy and Pharmaceutical Sciences, Josai University, 1-1 Keyaki-dai, Sakado, Saitama 350-0295, Japan*

[b]*Department of Chemistry, Faculty of Science, Josai University, 1-1 Keyaki-dai, Sakado, Saitama 350-0295, Japan*

* To whom correspondence should be addressed. Tel: +81-49-271-7256; E-mail: kamauchi@josai.ac.jp

SUMMARY

Twenty natural-product-like 2,8-dioxabicyclo[3.3.1]nonane derivatives were synthesized and their neuroprotective activities were tested using human monoamine oxidases (MAO) A and B and acetyl and butyryl cholinesterases (ChE). Compound **1s** showed inhibitory activity for MAO-A, MAO-B and AChE (IC_{50} values 34.0, 2.3 and 11.0 μM, respectively). The inhibition mode of (−)-**1s** for MAO-B was investigated. Chiral HPLC of (±)-**1s** separated the enantiomers and (−)-**1s** showed MAO-B inhibitory activity. Molecular docking simulation of (−)-**1s** and MAO-B revealed the binding mode.

KEYWORDS

Sanctis, 2,8-Dioxabicyclo[3.3.1]nonane, Lichen, Monoamine oxidase, Chiral HPLC

1 **GRAPHICAL ABSTRACT**

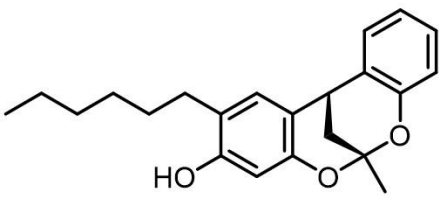

(−)-**1s**

IC_{50} (MAO-B) 0.90 μM

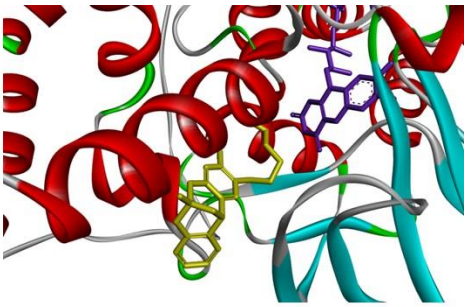

2

3

INTRODUCTION

Polyketide dimers, sanctis A and B (**1a** and **1b**), were isolated from the lichen *Parmotrema sancti-angelii* (Fig. 1).[1)] Sanctis have an unique carbon framework comprising a dibenzo-2,8-dioxabicyclo[3.3.1]nonane (DDN) scaffold and are biosynthesized from aromatic polyketide and chromene through nucleophilic attack, followed by intermolecular acetal closure. The total synthesis of sanctis A and B (**1a** and **1b**) was achieved by Tan's group in 2020, leading to a revision of the structure of sancti B and renaming of the original structure of sancti B to *iso*-sancti B (**1c**).[2)] Procyanidin A2 (**2**), an oligomeric compound comprising catechin and epicatechin, also has a DDN scaffold and exhibits antioxidant, antibacterial and glucose homeostasis preventive activities.[3)-5)]

Alzheimer's disease (AD) is one of the most common and devastating neurodegenerative diseases. The pathogenesis of AD is very complex. The many hypotheses regarding its pathogenesis suggest that the development of a multi-target-directed-ligand could be an effective therapeutic strategy.[6)] An important class of enzymes related to the etiology of AD is the monoamine oxidases (MAOs), which have two functional isozymic forms (MAO-A and MAO-B). MAO-B levels are significantly increased in the cerebral cortex and hippocampus of AD patients, accompanied by the increased production of hydrogen peroxide and reactive oxygen species.[7)] We previously reported bioactive orcinol derivatives targeted for AD. These derivatives consisted of orcinol with an alkyl side chain and showed a neuroprotective effect through their MAO-B inhibitory activity.[8)] Acetylcholinesterase (AChE) is the classic target of the cholinergic hypothesis, and most AD drugs currently on the market.[9)] As alzheimer's disease progresses, ChE activity declines, and relatively butyrylcholinesterase (BChE) activity increases. BChE, like ChE, also degrades acetylcholine. Therefore, by inhibiting BChE can be improve Alzheimer's disease as well

as AChE inhibitor. [10] Three AChE inhibitors (rivastigmine, donepezil, and galantamine) are approved for clinical use and rivastigmine represents an irreversible inhibitor for AChE and BChE respectively.

Sanctis A and B are DDN derivatives containing an orcinol moiety. Therefore, derivatives based on the structure of sanctis are expected to exhibit neuroprotective activity. In this study, DDN derivatives were synthesized and their neuroprotective activities were evaluated.

RESULT AND DISCUSSION

Synthesis of the DDN derivatives was achieved according to the total synthesis of sancti A (**1a**) and *iso*-sancti B (**1c**) (Scheme 1).[2] Hemiacetalization and dehydration of α,β-unsaturated carbonyl compounds (**3**) and a formal [3 + 3] cycloaddition cascade reaction with phenol derivatives (**4**) generated DDN derivatives (**1**). α,β-Unsaturated carbonyl intermediate **3a**, a common intermediate for sanctis, was prepared from commercially available orcinol in five steps (Scheme S1). Formylation, oxidation and methylation of orcinol yielded orsellinic acid methyl ester.[8] The α,β-unsaturated carbonyl structure was introduced by formination and Wittig reaction.[2] We also prepared two α,β-unsaturated carbonyl intermediates (**3b** and **3c**) by Wittig reaction and aldol condensation from *o*-vanillin and salicylaldehyde.

The ^{1}H-NMR signal of a deshielded methine proton at H-7 (δ_H 4.0–4.6 ppm, $J_{H\text{-}7\text{–}H\text{-}8} \fallingdotseq 3.0$ Hz) and a diastereotopic methylene group at H-8 (δ_H 2.0–2.2 ppm, $J_{H\text{-}7\text{–}H\text{-}8} \fallingdotseq 3.0$ Hz) suggested the presence of the DDN scaffold. The structural derivatization was introduced by using simplified α,β-unsaturated carbonyl intermediates (**3b** and **3c**) and alkyl phenols with various side chains.

Almost all [3 + 3] cycloaddition cascade reactions provided only a main regioisomer except using **3a** and **3c** with orcinol. Two regioisomers that could be separated by silica gel column

chromatography, yielding **1c** and **1p** as the main products. In contrast, the reaction of **3b** with orcinol generated two derivatives (confirmed by TLC analysis) but the main product could not be isolated due to the presence of non-separable by-products. The chemical shift of the methyl group helped us identify the position of the methyl group at C-12 or C-14. The methyl group of the main product was substituted at C-12 and the chemical shift appeared around δ_H 2.40 whereas the chemical shift of the minor product was around δ_H 2.10. The methyl proton at δ_H 2.15 suggested that **1n** has a methyl group at C-14.

The AChE and BChE inhibitory activities of the synthesized DDN derivatives were evaluated. **1s** showed AChE inhibitory activity and the IC_{50} value was 11 μM. The BChE inhibition test showed that two compounds (**1c** and **1e**) at 100 μM were active, with IC_{50} values of 47 and 11 μM, respectively (Table 1). The MAO-A and MAO-B inhibitory activities of the synthesized compounds were further evaluated using kynuramine, a substrate of MAO-A and MAO-B, and the amount of quinolinol produced was measured. Of the synthesized derivatives, four compounds (**1o**, **1p**, **1r** and **1s**) showed inhibitory activity for MAO-A, with IC_{50} values of 53, 28, 60 and 34 μM, respectively). In the MAO-B inhibition test, **1a**, **1r** and **1s** were active (IC_{50} values of 47, 23 and 2.3 μM, respectively) (Table 1). Compounds with less than 50% inhibition at 100 μM in each test were not listed in Table 1.

In natural products (**1a** and **1c**), **1a** showed only weak inhibitory activity against MAO-B and **1c** against BChE, respectively. On the other hand, several DDN derivatives showed stronger inhibitory activity than natural products, indicating that the combination of substituents C-1 to C-4 and C-12 to C-15 is important for activity expression. In the derivatives **1a**–**7i** commonly had the substituent at C-1 to C-4 with sancti A and B, only **1a** showed weak MAO-B inhibitory activity. The other active compounds don't have the substituents at C-1 to C-4 and **1r** and **1s** inhibited

MAO-B activity stronger than **1a**. Therefore, no substitution at C-1 to C-4 was preferred to show inhibitory activity in the MAO-B test. Then all compounds that showed inhibitory activity for MAO-A and MAO-B have hydroxy group at C-14 that is commonly presented in sancitis A and B. Next, we focused on the presence of the carbon side chain at C-13 on the inhibition. A butyl or hexyl sidechain at C-13 (**1r** and **1s**) resulted in inhibitory activity, with longer side chains being more effective for inhibit MAO-A and MAO-B. Absence of a side chain at C-13 (**1t**) resulted in no inhibition of MAO-A and MAO-B activity, suggesting that the carbon side chain at C-13 is necessary for inhibition. Comparison of **1l** and **1m** and active compounds **1r** and **1s** indicated that the presence of an *O*-methyl group at C-1 prevented inhibitory activity.

Derivative **1s** was the most promising lead compound among these synthesized compounds and showed MAO-A, MAO-B and AChE inhibition and evaluated as its racemic form. The chemical space of each optically active form was different. (+)-**1s** and (−)-**1s** were isolated by chiral phase HPLC of (±)-**1s**. Single-crystal X-ray crystallography suggested that the absolute configuration at C-7 and C-9 of (−)-**1s** is 7*S* and 9*R*, respectively (Fig. 4).[11),12)] Conversely, the absolute conformation of the enantiomer (+)-**1s** is 7*R*9*S*. The MAO-B assay using these enantiomers indicated that only (−)-**1s** showed inhibitory activity (IC_{50} value of 0.90 μM) (Table 2). The kinetics of (−)-**1s** towards MAO-B was investigated due to its remarkable inhibitory activity. Lineweaver−Burk plots of the inhibitory activities of (−)-**1s** towards MAO-B indicated that it is a competitive inhibitor (Fig. 2). Plotting the IC_{50} values at different substrate concentrations indicated that (−)-**1s** shows a linear correlation between IC_{50} value and substrate concentration (Fig. 3).

A molecular docking study was performed to investigate the mode of binding of (−)-**1s**. Affinity was evaluated by calculating the stability of the ligands when docked with the binding pocket of

the published MAO-B crystal structure (PDB 4A79)[13] using Auto Dock 4.2.[14] The molecular interactions of (−)-**1s** in the binding pocket include hydrogen bonding with Cys 172 and Ile 198, π–π interaction with Tyr 326, and π–σ interaction with Leu 171, Ile 199 and Ile 316. Alkyl–alkyl interactions were expected in the pendant methyl unit at C-9 with Trp 119, Leu 164, Leu 167 and Phe 168 and of the hexyl side chain with Tyr 326, Tyr 398 and Tyr 435 (Fig. 5).

CONCLUSION

In summary twenty DDN derivatives were synthesized by hemiacetalization, dehydration and formal [3 + 3] cycloaddition cascade reaction. Neuroprotective assays using the synthesized derivatives focused on MAOs and ChEs. The results showed that (±)-**1s** is a potential multi-inhibitor for MAOs and ChEs. Importantly, the inhibition of MAO-B by (±)-**1s** was equivalent to that of the positive control. Chiral resolution revealed that the active compound in the racemic mixture was (−)-**1s** and that the chemical space depended on the absolute configuration of the DDN scaffold.

EXPERIMENTAL

General Experimental Procedures

All reagents and solvents were purchased from commercial suppliers and used without further purification. Melting points were determined on a MP apparatus (Yanaco Technical Science Corp., Tokyo, Japan). Optical rotation was measured with a P-2000 polarimeter (Jasco Corp., Tokyo, Japan). 1D and 2D NMR spectra were measured at 298 K with a Varian 400-MR (400 MHz) spectrometer (Agilent Technologies Japan, Ltd., Tokyo, Japan) and a Bruker Avance NEO 400 MHz spectrometer (Bruker Japan K.K., Kanagawa, Japan) using tetramethylsilane as the internal

standard. Low- and high-resolution EI and FABMS spectra were measured with a JMS-700 spectrometer (JEOL, Tokyo, Japan). Column chromatography was performed using Wakogel C-200 (FUJIFILM Wako Pure Chemical Corporation, Osaka, Japan). Preparative HPLC was performed on a Jasco PU-4580 equipped with a Jasco UV-4570 detector (Jasco Corp.) at 254 nm. HPLC column was CHIRALPAK IE column (ϕ10 × 250 mm, 5 μm, Daicel Corp., Osaka, Japan). X-ray diffraction measurements were performed at 90 K on a Bruker D8 Venture diffractometer equipped with a PHOTON II detector with Cu Kα radiation (λ = 1.541780 Å, Bruker Japan K.K., Kanagawa, Japan).

Typical Synthetic Procedure of DDN derivatives *α,β*-Unsaturated carbonyl intermediates **3a-3c** were prepared according to the literature (Scheme S1). The general procedures for hemiacetalization, dehydration and formal [3 + 3] cycloaddition cascade reaction of the *α,β*-unsaturated carbonyl intermediate provided the *α,β*-unsaturated carbonyl intermediate (**3a-3c**) by following the literature.[2] Phenol derivatives **4** (2.1 eq) and *α,β*-unsaturated carbonyl intermediate **3a-3c** (1.0 eq) were dissolved in toluene (1.0 mL) and *p*-toluenesulfonic acid (PTSA, 0.1 eq) was then added. The resulting mixture was stirred for 2 h at 90°C and extracted using EtOAc-H_2O. The organic layer was dried over Na_2SO_4 and purified by silica-gel column chromatography (*n*-Hex-EtOAc) to yield DDN derivatives (**1**).

AChE and BChE Inhibitory assay

AChE and BChE inhibitory activities were assayed using the method in our previous report. [15)] 2 μL of cinnamic acid derivatives dissolved in DMSO, 6 μL of 0.06 mg/mL acetylthiocholine or 0.12 mg/mL butyrylthiocholine dissolved in 0.1 M phosphate buffer (pH 8.0), 180 μL of the buffer, 6 μL of 0.3 mM DTNB dissolved in the buffer, 6 μL of 0.15 U/mL AChE or 0.075 U/mL BChE dissolved in the buffer were added and mixed in a 96-well plate. The enzyme activity was

determined as the change in absorbance at 412 nm every 5 min during 30 min with a micro-plate reader (Molecular Devices SPECTRA MAX M2). The sample solution was replaced with DMSO as a control. Neostigmine was used as positive control.

MAO-A and -B inhibitory assay

MAO-A and MAO-B inhibitory activities were assayed using the method in the literature with slight modification.[16] 3 μL of human recombinant MAO-A solution (M7316, Sigma-Aldrich, St. Louis, MO) or 7 μL of MAO-B solution (M7441, Sigma-Aldrich) was diluted with 1100 μL of potassium phosphate buffer (0.1 M, pH 7.4). 140 μL of potassium phosphate buffer, 8 μL of kynuramine (final concentration is 30 μM, Sigma-Aldrich) in potassium phosphate buffer, and 2 μL of a dimethyl sulfoxide (DMSO) inhibitor solution (final DMSO concentration of 1% (v/v)), were mixed and pre-incubated at 37°C for 10 min. 50 μL of diluted MAO-A or MAO-B solution was then added to each well. The reaction mixture was further incubated at 37°C and the reaction was stopped after 20 min by the addition of 75 μL of 2 M NaOH. The product generated by MAO-A or MAO-B, 4-quinolinol, is fluorescent and was measured at Ex 310 nm/Em 400 nm using a microplate reader (SPECTRA MAX M2, Molecular Devices, Tokyo, Japan). DMSO without test compound was used as the negative control, and pargyline (Sigma-Aldrich) was used as a positive control. The IC_{50} values were estimated using Prism software (version 5.02; GraphPad, San Diego, CA). Pargyline was used as positive control.

Lineweaver−Burk plotting

This analysis was conducted according to the method reported by Meiring *et al.*[17] The inhibition of MAO-B by (−)-**1s** was determined by constructing a set of five Lineweaver–Burk plots. The first plot was constructed in the absence of inhibitor and the remaining four plots were constructed

in the presence of various concentrations of the test inhibitor. The enzyme substrate kynuramine was used at concentrations ranging from 7.5 to 480 μM.

CONFLICT OF INTEREST

The authors declare no conflict of interest.

SUPPLEMENTARY MATERIALS

This article contains supplementary materials.

REFERENCES

1) Duong TH., Ha XP., Chavasiri W., Beniddir MA., Genta-Jouve G., Boustie J., Chollet-Krugler M., Ferron S., Nguyen HH., Yamin BM., Huynh BLC., Pogam PL., Nguyen KPP., *European J. Org. Chem.,* **19**, 2247–2253 (2018).

2) Huo L., Dong C., Wang M., Lu X., Zhang W., Yang B., Yuan Y., Qiu S., Liu H., Tan H., *Org Lett.,* **22**, 934–938 (2020).

3) Dong XQ., Zou B., Zhang Y., Ge ZZ., Du J., Li CM., *Fitoterapia*, **97**, 128–139 (2013).

4) Gregoire S., Singh AP., Vorsa N., Koo H., *J. Appl. Microbiol.,* **103**, 1960–1968 (2007).

5) Ahangarpour A., Afshari G., Mard SA., Khodadadi A., Hashemitabar M., *J Physiol. Pharmacol..* **67**, 243–252 (2016).

6) Albertini C., Salerno A., de Sena Murteira Pinheiro P., Bolognesi ML., *Med. Res. Rev.,* **41**, 2606–2633 (2021).

7) Xu Y., Zhang J., Wang H., Mao F., Bao K., Liu W., Zhu J., Li X., Zhang H., Li J., *ACS Chem. Neurosci*., **10**, 482–496 (2019).

8) Kamauchi H., Oda T., Horiuchi K., Takao K., Sugita Y., S, *Bioorg. Med. Chem.,* **28**, 115156 (2020).

9) Wang N., Liu W., Zhou L., Liu W., Liang X., Liu X., Xu Z., Zhong T., Wu Q., Jiao X., Chen J., Ning X., Jiang X., Zhao Q., *ACS Omega.,* **7**, 32131–32152 (2022).

10) Darras FH., Kling B., Heilmann J., Decker M., *ACS Med. Chem. Lett.* **3**, 914–919 (2012).

11) Sheldrick GM., *Acta Cryst.,* **64**, 112–122 (2008).

12) Flack HD., Bernardinelli G., *J. Appl. Crystallogr.*, **33**, 1143–1148 (2000).

13) Binda C., Aldeco M., Geldenhuys WJ., Tortorici M., Mattevi A., Edmondson Dale E., *ACS Med. Chem. Lett.,* **3**, 39–42 (2012).

14) Cosconati S., Forli S., Perryman AL., Harris R., Goodsell DS., Olson AJ., *Expert. Opin. Drug Discov.*, **5**, 597–607 (2010).

15) Takao K., Kubota Y., Kamauchi H., Sugita Y., *Bioorg. Chem.,* **83**,432–437 (2019).

16) Novaroli L., Reist M., Favre E., Carotti A., Catto M., Carrupt PA., *Bioorg. Med. Chem*., **13**, 6212–6217 (2005).

17) Meiring L., Petzer JP., Petzer A., *Bioorg. Med. Chem. Lett.,* **23**, 5498–5502 (2013).

Figure legends

Fig. 1 Structures of DDN derivatives.

Fig. 2 X-ray crystal structure of (−)-**1s**.

Fig. 3 Lineweaver−Burk plot for MAO-B inhibition by (−)-**1s**.

Fig. 4 Effect of substrate (S) concentration on the IC_{50} value of (−)-**1s**.

Fig. 5 Molecular docking of (−)-**1s** and MAO-B. (a) Predicted binding conformations. (b) The key residues and their interactions with (−)-**1s**.

Scheme legends

Scheme 1 Synthesis of DDN derivatives.

Table legends

Table 1 Neuroprotective activities of the synthesized compounds.

Table 2 MAO-B inhibitory activities of (+)-**1s** and (−)-**1s**.

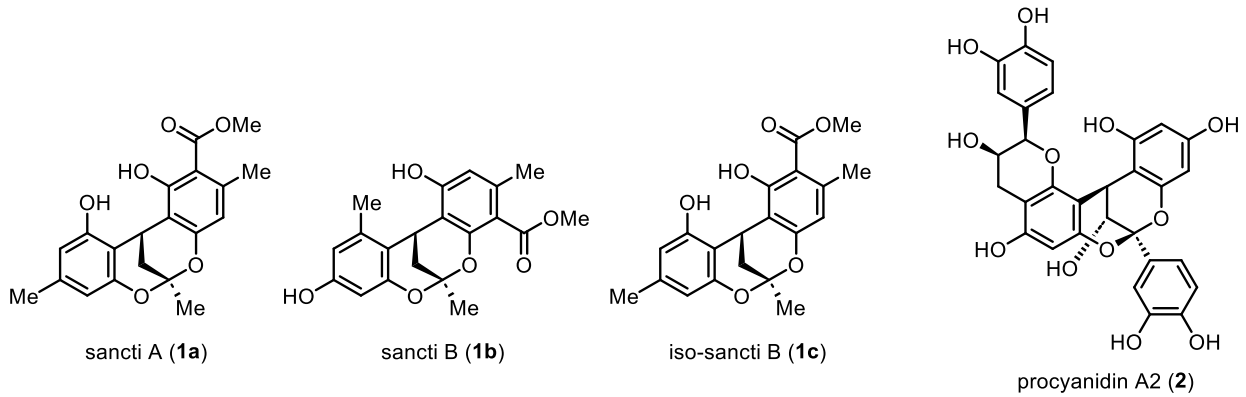

1

2 Figure 1 Structures of DDN derivatives.

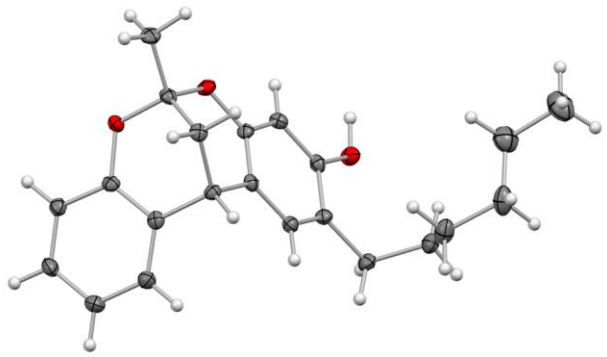

3

4 Figure 2 X-ray crystal structure of (−)-**1s**.

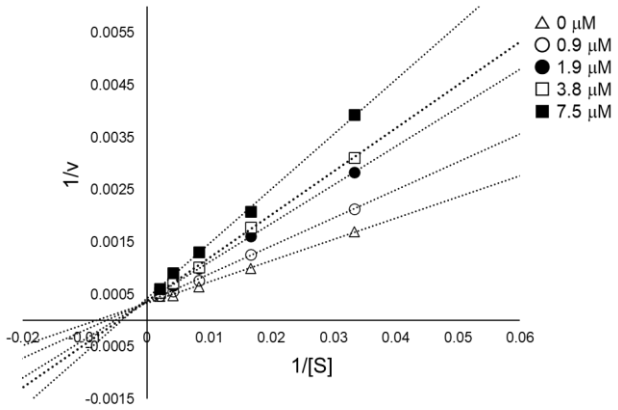

5 Figure 3 Lineweaver−Burk plot for MAO-B inhibition by (−)-**1s**.

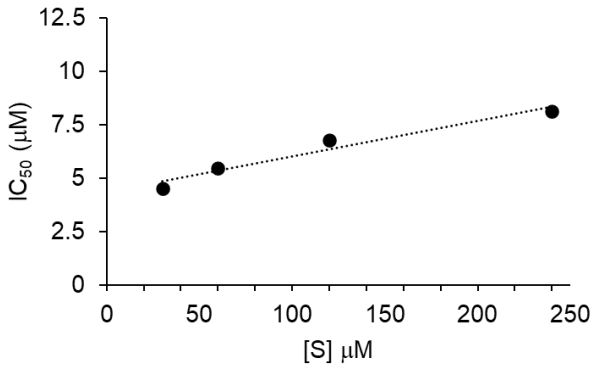

Figure 4 Effect of substrate (S) concentration on the IC_{50} value of (−)-**1s**.

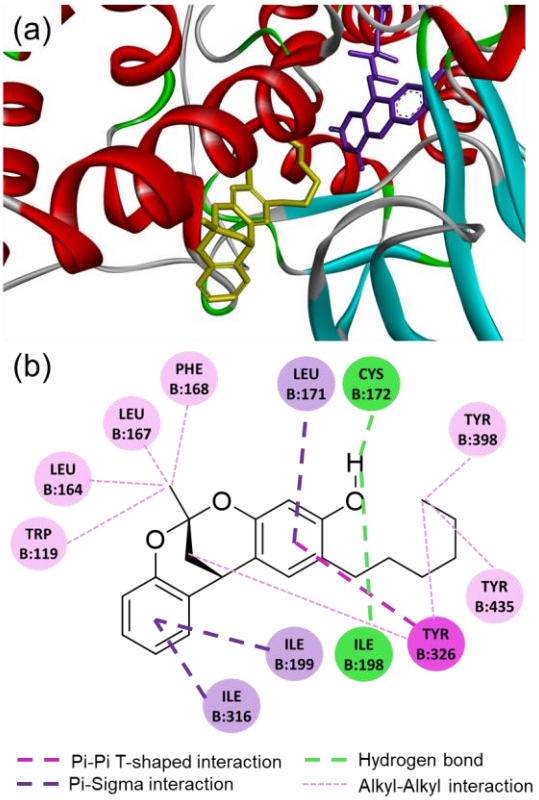

Figure 5 Molecular docking of (−)-**1s** and MAO-B. (a) Predicted binding conformations. (b) The key residues and their interactions with (−)-**1s**.

Table 1 Neuroprotective activities of the synthesized compounds.

AChE (IC_{50}, μM)	
1s	11
Neostigmine	0.20

BChE (IC_{50}, μM)	
1c	47
1e	11
Neostigmine	7.1

MAO-A (IC_{50}, μM)	
1o	53
1p	28
1r	60
1s	34
Pargyline	4.0

MAO-B (IC_{50}, μM)	
1a	47
1r	23
1s	2.3
Pargyline	1.5

Table 2 MAO-B inhibitory activities of (+)-**1s** and (−)-**1s**.

MAO-B (IC_{50}, μM)			
(+)-**1s**	>25	(−)-**1s**	0.90

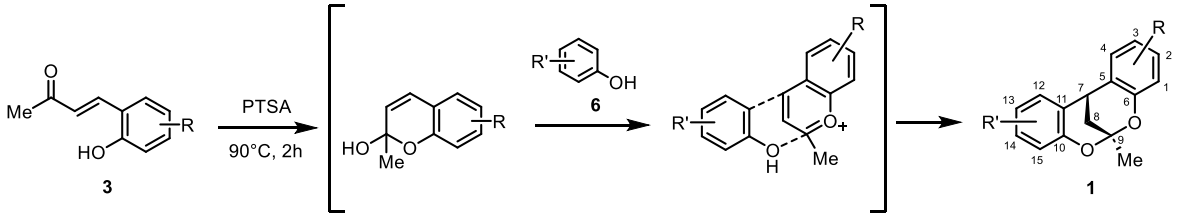

starting materials	adducts (**4**)	products (**1**)						
				R^1	R^2	R^3	R^4	yield (%)
3a			**1a**	OH	H	Me	H	6
			1c	Me	H	OH	H	16
			1d	Me	H	OH	OH	65
			1e	Me	farnesyl	OH	H	19
			1f	H	Et	OH	H	22
			1g	H	*n*-Bu	OH	H	68
			1h	H	*n*-Hex	OH	H	74
			1i	H	H	OH	H	47
3b			**1j**	Me	H	OMe	H	27
			1k	H	Et	OH	H	2
			1l	H	*n*-Bu	OH	H	68
			1m	H	*n*-Hex	OH	H	63
			1n	OH	H	Me	H	16
3c			**1o**	OH	H	Me	H	11
			1p	Me	H	OH	H	36
			1q	H	Et	OH	H	80
			1r	H	*n*-Bu	OH	H	77
			1s	H	*n*-Hex	OH	H	68
			1t	H	H	OH	H	62
			1u	Me	H	OMe	H	33

Scheme 1 Synthesis of DDN derivatives.